



Cite this: *Polym. Chem.*, 2023, **14**, 1103

## Palladium-catalyzed synthesis of oil-based functionalized polyolefins†

Jiawei Chen,<sup>‡a</sup> Wenbing Wang,<sup>‡a</sup> Yao Pan,<sup>a</sup> Dan Peng,<sup>\*a</sup> Yougui Li<sup>\*b</sup> and Chen Zou<sup>ID</sup><sup>\*a</sup>

The fabrication of functionalized polyolefin materials from renewable biomass is of great importance for sustainable development. In this study, we achieved direct copolymerization of plant oil-based copolymer monomers with ethylene using a dienyl phosphoribosulfonyl palladium catalyst (PO-Pd). Ureido-pyrimidinone (UPy) functionalization was also performed using the hydroxyl group of the polymer. The incorporation of biomass groups can effectively modulate the surface and mechanical properties of the copolymers, and more importantly, these newly developed polymers are ideal tougheners for gutter oil. The excellent tunability of the self-complementary hydrogen bonding network (UPy) allows the achievement of a range of interesting mechanical properties including self-reinforcement and high mechanical damping. This strategy establishes the groundwork for further research into value-added applications of plant oils and encourages new applications in the field of multifunctional smart materials.

Received 4th January 2023,  
Accepted 3rd February 2023

DOI: 10.1039/d3py00012e

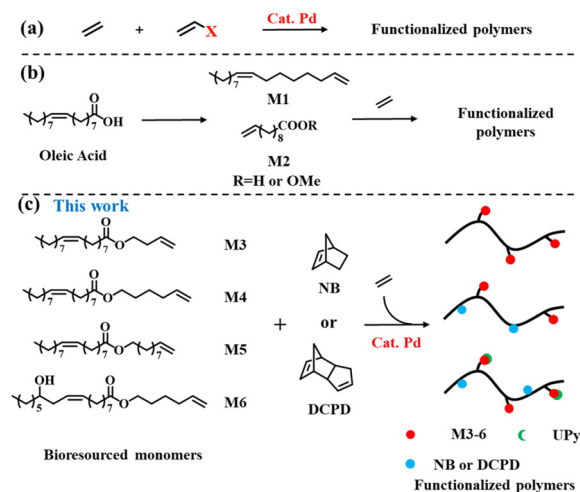
rsc.li/polymers

### Introduction

Polyolefins are widely used as commodity plastics because of their many excellent properties.<sup>1</sup> However, their non-polar nature has become one of their biggest limitations.<sup>2–5</sup> Late transition metal-catalyzed copolymerization of olefins with polar copolymer monomers is an efficient and alluring method of introducing functional groups that can enhance the properties of polyolefins and widen the application range of functionalized polyolefins.<sup>6–24</sup> For example, recently, the copolymerization of ethylene with various polar copolymer monomers has been extensively explored using phosphine sulfonates and related palladium catalysts, and a series of properties (such as viscosity, surface properties, and dyeing and mechanical properties) of polar functionalized polyolefin materials have been studied on this basis (Scheme 1a).<sup>25–33</sup>

However, most of these monomers used to prepare functional polyolefin materials come from non-renewable petroleum resources,<sup>34</sup> and only a few biomass converted monomers are used for olefin polymerization.<sup>28,29,35–38</sup> At present,

due to the depletion of fossil resources and environmental damage, bio-based polymers are considered as potential candidates for future polymer applications.<sup>38,39</sup> Among the various renewable resources, plant oils and their derivatives are gaining popularity in the field of polymer synthesis.<sup>40–43</sup> For example, Kanbara *et al.* performed the decarbonyl elimination of fatty acids under Pd catalysis to obtain the corresponding



**Scheme 1** (a) Palladium-catalyzed copolymerization of ethylene with a polar comonomer. (b) The bioresourced monomers copolymerized with ethylene. (c) Fabrication of novel polyolefin materials from renewable biomass.

<sup>a</sup>CAS Key Laboratory of Soft Matter Chemistry, Hefei National Laboratory for Physical Sciences at the Microscale, Department of Polymer Science and Engineering, University of Science and Technology of China, Hefei, 230026, China.

E-mail: chen1215@ustc.edu.cn, pengdan@mail.ustc.edu.cn

<sup>b</sup>School of Chemistry and Chemical Engineering, Hefei University of Technology, Hefei 230009, China. E-mail: liyg1224@126.com

† Electronic supplementary information (ESI) available. See DOI: <https://doi.org/10.1039/d3py00012e>

‡ These authors contributed equally.



**Scheme 2** (a) Palladium-catalyzed copolymerization of ethylene with a polar comonomer. (b) The bioresourced comonomers copolymerized with ethylene. (c) Schematic diagram of P-HEO toughened HDPE/gutter oil. (d) A polyolefin protective gear schematic with complementary hydrogen bonding interactions.

$\alpha$ -olefins, and used Zr catalysts for polymerization to obtain a new functional polyolefin.<sup>44</sup> In the field of late transition metal catalysts, Chen *et al.* used bulky  $\alpha$ -diimine palladium catalysts to catalyze the copolymerization of ethylene with 10-undecenoic acid and its ester (Scheme 1b) extracted from castor oil to prepare a functionalized polyethylene thermoplastic elastomer, a polar monomer, up to 3.8% at the expense of molecular weight ( $M_n = 1.1700 \text{ g mol}^{-1}$ ).<sup>36</sup>

In this study, we converted oleic acid or castor oil acid into a functional olefin monomer, and prepared a series of plant oil-derived functional polyolefins with excellent mechanical properties and surface properties by the copolymerization of ethylene with these functional olefin monomers using the palladium phosphine sulfonate catalyst PO-Pd (Schemes 1c and 2b). We further mixed these functionalized polyolefins with various plant oils to prepare high-performance composites, expecting to recover kitchen waste oil (Scheme 2c). The functional polyolefin material with damping properties was prepared by introducing multiple hydrogen bonds (Schemes 2b and d) after functional group modification and utilizing the dynamic crosslinking properties of UPy.

## Results and discussion

### Comonomer synthesis

Various halogen monomers (4-bromo-1-butene, 6-bromo-1-hexene, and 10-bromo-1-decene monomers) were used as raw materials to react with oleic and ricinoleic acids to generate fatty acid-based monomers, yielding products named BEO, HEO, DEO, and CEO, respectively. These plant oil-based monomers can be easily synthesized by a simple and efficient inter-esterification reaction between carboxyl and halide under the catalysis of 1,1,3,3-tetramethylguanidine (TMG) (Scheme 2a).

In this work, a biaryl-substituted phosphine-sulfonate palladium (PO-Pd) catalyst was selected because of its high tolerance toward polar functional groups and its ability to generate high-molecular weight polyethylene (Table 1, entry 1). The characteristic peaks of the monomers (such as  $\text{COOCH}_2$  groups) are clearly known from the results of the NMR characterization of these copolymers. Fig. S6–15† demonstrate the successful insertion of polar monomers. The polymerization activity, comonomer incorporation and the molecular weight of copolymer P-BEO in the presence of large amounts of the

**Table 1** Ethylene copolymerization studies with the PO-Pd catalysts<sup>a</sup>

Ent.	Comonomer1 ([M])	Comonomer2 ([M])	Yield (g)	Act. <sup>b</sup>	Incorp1./Incorp2. <sup>c</sup> (%)	T <sub>g</sub> /T <sub>m</sub> <sup>d</sup> (°C)	M <sub>n</sub> (10 <sup>4</sup> ) <sup>e</sup>	PDI <sup>e</sup>
1	—	—	3.8	38	—	—/123.7	20.9	1.8
2	BEO (1 M)	—	2.5	25	0.4	—/127.9	17.5	2.4
3	HEO (1 M)	—	3.2	32	1.2	—/125.4	16.6	3.2
4	DEO (1 M)	—	2.8	28	0.9	—/120.7	11.5	4.4
5	CEO (1 M)	—	3.0	30	0.9	—/115.6	13.6	3.4
6	HEO (0.5 M)	NB (0.5 M)	3.5	35	0.8/6.5	—/109.9	10.5	4.6
7	HEO (0.5 M)	NB (1 M)	3.8	38	0.8/12.5	-11.3/53.0	10.4	3.1
8	HEO (1 M)	NB (0.5 M)	3.1	31	1.0/7.2	—/78.0	6.9	2.6
9	HEO (0.5 M)	DCPD (1 M)	3.3	33	0.5/5.5	—/86.0	14.5	2.5
10	HEO (1 M)	DCPD (1 M)	3.6	36	1.3/6.5	—/83.5	7.8	2.6
11	CEO (1 M)	NB (0.5 M)	3.5	35	2.0/5.0	—/120.2	6.1	4.8

<sup>a</sup> Conditions: 10 μmol catalyst in 2 ml CH<sub>2</sub>Cl<sub>2</sub>; 30 mL total volume of toluene and the comonomer; T = 80 °C; ethylene pressure (atm) = 8 atm; time = 1 h. <sup>b</sup> Activity = 10<sup>4</sup> g<sub>polymer</sub> mol<sub>pd</sub><sup>-1</sup> h<sup>-1</sup>. <sup>c</sup> Comonomer incorporation ratio was determined by <sup>1</sup>H NMR in C<sub>2</sub>D<sub>2</sub>Cl<sub>4</sub> at 120 °C. <sup>d</sup> Determined by DSC. <sup>e</sup> Determined by GPC in trichlorobenzene at 150 °C.

BEO copolymer monomer (1.0 mol L<sup>-1</sup>) were 2.5 × 10<sup>5</sup> g mol<sup>-1</sup> h<sup>-1</sup>, 0.4% and 175 000 g mol<sup>-1</sup>, respectively (Table 1, entry 2). The polymerization activities of copolymers P-HEO, P-DEO and P-CEO also reached about 3.0 × 10<sup>5</sup> g mol<sup>-1</sup> h<sup>-1</sup> (Table 1, entries 3–5), and the molecular weights of P-HEO, P-DEO and P-CEO were similar to that of P-BEO with 166 000, 115 000 and 136 000 g mol<sup>-1</sup>, respectively. The terpolymers exhibit diverse and comprehensive properties. Surprisingly, the activity, incorporation, and the molecular weight of the terpolymers did not significantly decrease with the addition of the polar copolymer monomers NB and DCPD. The comonomer incorporation of terpolymer P-HEO/NB 0.5 M/0.5 M, 0.5 M/1.0 M and 1.0 M/0.5 M reached 0.8/6.5%, 0.8/12.5% and 1.0/7.2%, respectively (Table 1, entries 6–8). The comonomer incorporation increases significantly with increasing comonomer concentration. The palladium catalyst still showed high polymerization activity (3.3–3.6 × 10<sup>5</sup> g mol<sup>-1</sup> h<sup>-1</sup>) and comonomer incorporation (5.5–6.5%) with the introduction of the DCPD monomer compared to NB (Table 1, entries 9 and 10). In addition, for the castor oil-based monomer COE, the terpolymers can also be prepared with high activity up to 3.5 × 10<sup>5</sup> g mol<sup>-1</sup> h<sup>-1</sup> (Table 1, entry 11). The use of plant oil-based copolymer monomers provides maximal property tunability. The addition of NB and DCPD enhances chain unit flexibility, converting the copolymer to an elastomer.

### Mechanical properties

The effect of plant oil-based monomers on the mechanical characteristics of the comonomer is discussed first (Fig. 1). The mechanical properties are closely related to the type of copolymer and the percentage of its incorporation. As shown in Fig. 1a, PE shows a tensile strength and an elongation at break of about 23 MPa and 530%, respectively. The tensile strength of P-BEO, P-HEO, P-DEO and P-CEO was 31, 34, 18 and 9 MPa, respectively. In addition, their elongation at break was about 850, 950, 810 and 530%, respectively. The introduction of plant oil-based monomers significantly improved the toughness of the copolymers. The majority of the copolymer samples obtained exhibit typical

plastic properties with significant yields. Compared to P-HEO, P-DEO and P-CEO, the yield strength and Young's modulus of P-BEO were increased to 19 and 250 MPa, respectively. The chain length of DEO disturbs the chain rule and tends to remain amorphous, while that of BEO favors the crystal microstructure. However, P-HEO showed better toughness at different levels of increased mechanical properties. This is attributed to the high insertion ratio of HEO. The introduction of NB and DCPD has endowed the terpolymer with diverse properties (Fig. 1b). The random copolymerization units of ethylene and plant oil-based monomers act as the "soft" units in these copolymers, while the polyethylene crystalline units act as the "hard" units, and these interactions may increase the copolymers' elastic and tensile properties. The tensile strength of DCPD-based polymers is significantly higher than that of NB-based polymers, which could be attributed to the differences in the polymer molecular weight and the monomer ring structure. The addition of the NB monomer reduces the tensile strength but does not affect the strain-at-break values. The strain-at-break value decreases as the HEO monomer insertion ratio decreases. The P-HEO/DCPD 0.5 M/1 M terpolymer has an incredible tensile strength of 46 MPa and a tensile elongation of 930%, making it an ultra-tough polyolefin elastomer.

### Surface properties

The surface properties of these polar functionalized polymers were investigated by measuring the copolymer's water contact angle. The hydrophilicity of the plant oil-based copolymers was significantly higher due to the introduction of polar groups compared to pure polyethylene, as shown in Fig. 1c. The contact angle of the copolymers decreased from 110° for pure polyethylene to 86.6° for the copolymers. Furthermore, the terpolymer water contact angle values decreased slightly with the addition of DCPD and NB. This is clearly an effective strategy for modulating/improving the surface properties of polyolefin materials.



**Fig. 1** (a and b) Stress–strain curves for selected copolymer and terpolymer samples. (c) Water contact angles for the polymer products. (PE: entry 1, P-BEO 1 M: entry 2, P-HEO 1 M: entry 3, P-DEO 1 M: entry 4, P-CEO 1 M: entry 5, P-HEO/NB: entries 6–8, P-HEO/DCPD: entries 9 and 10, P-CEO/NB: entry 11) (in the polymer nomenclature, the number after the comonomer represents its concentration during copolymerization or terpolymerization). Stress–strain curves of (d) HDPE/CO composites. SEM image of the liquid nitrogen quenched surfaces of (e) HDPE/CO 80/20 and (f) HDPE/CO/P-HEO-1 M 75/20/5. (g) Curves of stress and strain for HDPE blends with different plant oils: ESO, RO and TO. (h and i) Mechanical properties of the polymer samples after vulcanization.

## Blending recycling of waste cooking oil

Waste cooking oil is a renewable resource. Its reuse can effectively solve the problem of waste oil pollution. Polar functional groups, in addition to modulating the mechanical properties, can improve many other properties of polyolefin materials, such as miscibility with other polymers (Scheme 2c). The stress–strain curves of the copolymer-toughened HDPE/castor oil (CO) blends are shown in Fig. 1d. The HDPE/CO 80/20 blends manifest a typical brittle fracture behavior with the disappearance of elongation after yielding and the elongation at break is just 30%. It is surprising that the HDPE/CO/P-HEO 1 M 75/20/5 blend (with an addition of just 5 wt% P-HEO 1 M) shows an elongation at break at about 730%, which is about 23 times longer than that of the HDPE/CO 80/20 blend. The toughening effect of P-CEO 1 M is significant, but it has not yet achieved the mechanical properties of the HDPE/CO/P-HEO 1 M 75/20/5 blends. This may be due to the insertion ratio and the molecular weight of the copolymer.

The phase morphology of surfaces can be used to further indicate the existence of toughness during tensile deformation. SEM was applied to observe the fractured surfaces of HDPE/CO blends and their SEM micrographs are shown in Fig. 1e and f. Noticeably, the fractured surface of the HDPE/CO

blend showed significant phase separation, indicating a typical brittle failure of the HDPE/CO blend film. In contrast, the fractured surfaces of the HDPE/CO/P-HEO-1 M blends exhibit regular surface patterns.

We blended HDPE with various plant oils to demonstrate the generalizability of the copolymer blending toughening. Fig. 1g further shows that the elongation at break of HDPE/P-HEO 1 M and Epoxy Soybean Oil (ESO), Rapeseed Oil (RO), and Tung Oil (TO) 75/5/20 blends reached about 170%, 1170% and 1290%, respectively. The addition of P-HEO 1 M did not cause the blends' yield strength values to drop, and both the elongation at break and the yield strength of the HDPE/plant oil/P-HEO 1 M blends remained high.

Cross-linking reactions are well known for improving the mechanical, thermal, and physicochemical properties of a wide range of polymeric materials. As a result of the abundance of reactive groups in plant oils, such as double bonds, sulfur vulcanization can quickly and efficiently create robust cross-linked networks. The stress–strain curves in Fig. 1h show a significant increase in the tensile strength after cross-linking, and a significant increase in the strain to fracture and the elastic properties. The OH functional group in P-CEO also served as an active site for crosslinking, resulting in a tensile strength and tensile strain at break of 14 MPa and 990%,

respectively, for the crosslinked P-CEO 1 M/CO 80/20 blends. After cross-linking, the toughness of P-CEO 1 M/CO 80/20 reaches a maximum of  $86 \text{ MJ m}^{-3}$ , which is a 9 times increase (Fig. 1i).

### UPy functionalization and damping properties

The properties of these polar-functionalized polyolefins can be further improved/modified through postpolymerization functionalization. For example, the incorporated OH groups can be converted into other functional groups through known organic transformations. Polyolefin polymers with UPy units were synthesized by a two-step method. Monoisocyanato methylisocytosine (MIMIS) was first synthesized *via* the reaction of 2-amino-4-hydroxy-6-methylpyrimidine and hexamethylene diisocyanate (HDMI). Then polyolefin functionalized materials were prepared by the reaction of MIMIS with P-CEO 1 M or P-CEO/NB 1 M/0.5 M.

Supramolecular materials are dynamic materials in which supramolecular forces respond more strongly to external stimuli, resulting in changes in the fracture–reconstruction equilibrium. Among them, UPy has attracted a lot of attention because of its ability to form complementary quadruple hydrogen bonds with higher bond strengths than normal hydrogen bonds. Supramolecular materials are capable of exhibiting degradability, shape memory, self-healing, and damping by utilizing these properties. The tensile strength of P-CEO 1 M-UPy after UPy functionalization was 27 MPa, and the elongation at break was 1060%, both of which were significantly higher than the comparable P-CEO 1 M without any form of functionalization. The same pattern is visible in P-CEO/NB 1 M/0.5 M-UPy (Fig. 2a and b).

Since the polymers in P-CEO 1 M and P-CEO/NB 1 M/0.5 M are completely connected by stable covalent bonds, the polymer network topology does not change and exhibits

elastic properties. In contrast, after the addition of UPy, its polymer network is connected by partially reversible bonds (UPy dimer) and partially covalent bonds, and the copolymer's tensile strength and toughness are increased by the strong hydrogen bonding interactions. At room temperature the UPy dimer behaves as a solid elastomer (undergoes elastic deformation) due to its slow rate of exchange. However, as the temperature increases, the UPy dimer exchange rate becomes faster and the sample becomes more and more liquid in nature (plastic deformation). The rheological plots in Fig. 2c and d show that at higher temperatures, the energy storage moduli of P-CEO/NB 1 M/0.5 M and P-CEO/NB 1 M/0.5 M-UPy exhibit strong strain rate dependence. The samples are more liquid and behave more like a “non-Newtonian fluid”. The dynamic nature of UPy dimers opens up new possibilities for the design of mechanically lossy materials. We used the dropping the ball test to determine the mechanical loss of various samples, as shown in Fig. 2e and f. The position of the ball drop and the highest point of the next bounce were recorded using a camera. After bouncing, P-CEO/NB 1 M/0.5 M and P-CEO/NB 1 M/0.5 M-UPy small balls can still reach a relatively high position and exhibit good elasticity. The mechanical loss of P-CEO/NB 1 M/0.5 M-UPy is higher, especially at  $100^\circ\text{C}$ , and the height of the bouncing ball is significantly reduced, demonstrating excellent damping characteristics. Such mechanical loss is also caused by the dynamic exchange of UPy dimers. When the ball collides with the ground due to the impact of external forces, the energy exerted by the outside world causes the dissociation and reconstruction of the UPy dimer, which is part of the energy consumption. The more the UPy content, the stronger the energy dissipation capacity, and the damping characteristics are derived from this.



**Fig. 2** Effect of UPy on the mechanical properties of (a) P-CEO 1 M and (b) P-CEO/NB 1 M/0.5 M. Storage modulus curves in the frequency sweep experiments of P-CEO/NB 1 M/0.5 M (c) and P-CEO/NB 1 M/0.5 M-UPy (d) at different temperatures. Mechanical damping performance: (e) P-CEO/NB 1 M/0.5 M and (f) P-CEO/NB 1 M/0.5 M-UPy.

## Conclusions

In summary, PO-Pd effectively mediates the copolymerization of ethylene with monomers derived from plant oils. This system demonstrated high catalytic activity in the preparation of copolymers with high molecular weight and adjustable copolymerization monomer incorporation. Because of their polar nature and high elastic properties, these newly developed polymers are excellent candidates for use as toughening components in polymer blends. These have the potential to make gutter oil more valuable. CEO adds more active sites for functionalization, which can improve the mechanical and elastic properties. UPy's dynamic equilibrium nature results in a polymer network with unusual mechanical properties, such as good strain rate dependence and excellent mechanical damping. Different combinations of these properties can lead to new applications, and optimizing the dynamic exchange of UPy will broaden the range of polymer applications and provide greater application potential.

## Conflicts of interest

There are no conflicts to declare.

## Acknowledgements

This work was supported by the National Natural Science Foundation of China (NSFC 22101274 and 52203016) and the China Postdoctoral Science Foundation (2021M703072 and 2022T150617).

## References

- M. Sturzel, S. Mihan and R. Mulhaupt, *Chem. Rev.*, 2016, **116**, 1398–1433.
- T. M. Chung, *Functionalization of polyolefins*, Elsevier, 2002.
- N. M. Franssen, J. N. Reek and B. de Bruin, *Chem. Soc. Rev.*, 2013, **42**, 5809–5832.
- J. Y. Dong and Y. Hu, *Coord. Chem. Rev.*, 2006, **250**, 47–65.
- N. K. Boen and M. A. Hillmyer, *Chem. Soc. Rev.*, 2005, **34**, 267–275.
- Z. Chen and M. Brookhart, *Acc. Chem. Res.*, 2018, **51**, 1831–1839.
- A. Nakamura, T. M. Anselment, J. Claverie, B. Goodall, R. F. Jordan, S. Mecking, B. Rieger, A. Sen, P. W. Van Leeuwen and K. Nozaki, *Acc. Chem. Res.*, 2013, **46**, 1438–1449.
- L. Guo, S. Dai, X. Sui and C. Chen, *ACS Catal.*, 2016, **6**, 428–441.
- J. Chen, Y. Gao and T. J. Marks, *Angew. Chem.*, 2020, **132**, 14834–14843.
- C. Tan and C. Chen, *Angew. Chem.*, 2019, **131**, 7268–7276.
- A. Nakamura, S. Ito and K. Nozaki, *Chem. Rev.*, 2009, **109**, 5215–5244.
- H. Mu, G. Zhou, X. Hu and Z. Jian, *Coord. Chem. Rev.*, 2021, **435**, 213802.
- C. Tan, C. Zou and C. Chen, *Macromolecules*, 2022, **55**, 1910–1922.
- D. Takeuchi and K. Osakada, *Polymer*, 2016, **82**, 392–405.
- L. Guo and C. Chen, *Sci. China: Chem.*, 2015, **58**, 1663–1673.
- M. Baur, F. Lin, T. O. Morgen, L. Odenwald and S. Mecking, *Science*, 2021, **374**, 604–607.
- C. Chen, *Nat. Rev. Chem.*, 2018, **2**, 6–14.
- R. S. Birajdar and S. H. Chikkali, *Eur. Polym. J.*, 2021, **143**, 110183.
- S. Xiong, A. Hong, B. C. Bailey, H. A. Spinney, T. D. Senecal, H. Bailey and T. Agapie, *Angew. Chem., Int. Ed.*, 2022, **61**, e202206637.
- L. Odenwald, F. P. Wimmer, N. K. Mast, M. G. Schussmann, M. Wilhelm and S. Mecking, *J. Am. Chem. Soc.*, 2022, **144**, 13226–13233.
- C. Zou, G. Si and C. Chen, *Nat. Commun.*, 2022, **13**, 1954.
- Y. Zhang, H. Mu, L. Pan, X. Wang and Y. Li, *ACS Catal.*, 2018, **8**, 5963–5976.
- R. J. Witzke, A. Chapovetsky, M. P. Conley, D. M. Kaphan and M. Delferro, *ACS Catal.*, 2020, **10**, 11822–11840.
- G. Ji, Z. Chen, X. Y. Wang, X. S. Ning, C. J. Xu, X. M. Zhang, W. J. Tao, J. F. Li, Y. Gao, Q. Shen, X. L. Sun, H. Y. Wang, J. B. Zhao, B. Zhang, Y. L. Guo, Y. Zhao, J. Sun, Y. Luo and Y. Tang, *Nat. Commun.*, 2021, **12**, 6283.
- C. Zou and C. Chen, *Angew. Chem., Int. Ed.*, 2020, **59**, 395–402.
- C. Zou, H. Zhang, C. Tan and Z. Cai, *Macromolecules*, 2020, **54**, 64–70.
- C. Zou, W. Pang and C. Chen, *Sci. China: Chem.*, 2018, **61**, 1175–1178.
- Y. Na and C. Chen, *Angew. Chem., Int. Ed.*, 2020, **59**, 7953–7959.
- M. Chen and C. Chen, *Angew. Chem., Int. Ed.*, 2020, **59**, 1206–1210.
- M. Xu and C. Chen, *Sci. Bull.*, 2021, **66**, 1429–1436.
- J. Gao, W. Cai, Y. Hu and C. Chen, *Polym. Chem.*, 2019, **10**, 1416–1422.
- S. Takano, D. Takeuchi, K. Osakada, N. Akamatsu and A. Shishido, *Angew. Chem.*, 2014, **126**, 9400–9404.
- Z. Jian, L. Falivene, G. Boffa, S. O. Sánchez, L. Caporaso, A. Grassi and S. Mecking, *Angew. Chem.*, 2016, **128**, 14590–14595.
- R. W. Bentley, *Energy Policy*, 2002, **30**, 189–205.
- B. S. Rajput, S. B. Pawal, D. V. Bodkhe, I. N. Rao, A. V. S. Sainath and S. H. Chikkali, *Eur. Polym. J.*, 2020, **134**, 109775.
- S. Dai, S. Li, G. Xu and C. Chen, *Macromolecules*, 2020, **53**, 2539–2546.
- L. R. Parisi, D. M. Scheibel, S. Lin, E. M. Bennett, J. M. Lodge and M. J. Miri, *Polymer*, 2017, **114**, 319–328.
- C. Du, L. Zhong, J. Gao, S. Zhong, H. Liao, H. Gao and Q. Wu, *Polym. Chem.*, 2019, **10**, 2029–2038.

- 39 A. Gandini and T. M. Lacerda, *Prog. Polym. Sci.*, 2015, **48**, 1–39.
- 40 L. Yu, K. Dean and L. Li, *Prog. Polym. Sci.*, 2006, **31**, 576–602.
- 41 F. Stempfle, P. Ortmann and S. Mecking, *Chem. Rev.*, 2016, **116**, 4597–4641.
- 42 U. Biermann, U. Bornscheuer, M. A. Meier, J. O. Metzger and H. J. Schäfer, *Angew. Chem., Int. Ed.*, 2011, **50**, 3854–3871.
- 43 S. A. Miller, *ACS Macro Lett.*, 2013, **2**, 550–554.
- 44 K. Ohtake, Y. Onose, J. Kuwabara and T. Kanbara, *React. Funct. Polym.*, 2019, **139**, 17–24.